Indonesian Journal of Physics
Vol. 33. No.1, 17 October 2022
Journal homepage: http://ijphysics.com

Thermoelectrics of type-I and type-II nodal line semimetals within the two-band model

J. M. Adhidewata[1*], Ahmad R. T. Nugraha[2], E. H. Hasdeo[2,3], B. E. Gunara[1]
[1] *Theoretical High Energy Physics Research Division, Faculty of Mathematics and Natural Sciences, Institut Teknologi Bandung, Bandung 40132, Indonesia*
[2] *Research Center for Quantum Physics, National Research and Innovation Agency (BRIN), Tangerang Selatan 15314, Indonesia*
[3] *Department of Physics and Materials Science, University of Luxembourg, L-1511 Luxembourg, Luxembourg*

(Received: 28 February 2022, Revised: 30 May 2022, Accepted: 11 October 2022)

Abstract

Metals and semimetals are often considered poor thermoelectric (TE) materials due to their low Seebeck coefficients. However, we will show that topological semimetals in the class of nodal-line semimetals (NLSs) may potentially exhibit better performance as TE materials. The NLSs are semimetals with an intersection between the conduction band and valence band in the forms of a line (thus called the nodal line). We construct a two-band model using an almost-linear conduction and parabolic (or Mexican-hat) valence bands that overlap each other near the band edge to represent a type-I (or type-II) NLS. We calculate TE properties of the NLSs using the semiclassical Boltzmann transport theory and the relaxation time approximation. By varying the band parameters in our model, we find that the type-II NLS generally has better TE performance than the type-I NLS. The type-II NLS, in particular, possesses a Seebeck coefficient with a value possibly larger than twice that of normal metals. The origin of this feature might be the presence of a discontinuity in the density of states due to the intersection of the valence and conduction bands.

Keywords: Boltzmann transport theory, Mexican-hat band, nodal-line semimetal, thermoelectrics

INTRODUCTION

Recently there has been a lot of interest on materials with non-trivial band topology [1-5]. Example materials of interest are nodal line semimetals (NLSs) [1, 6]. The NLSs are semimetals where the conduction band and the valence band intersect in forms of a line, and thus called the nodal line [1, 6, 7]. We can classify the NLSs into type-I and type-II NLS based on the slope of the conduction and valence bands at the intersection line. In the type-I NLS, the slopes of the two bands align oppositely, while in the type-II NLSs, the two bands have the same slope direction along the nodal line [7, 8].

Metals and semimetals usually perform poorly as thermoelectric (TE) materials (i.e., to convert heat directly into electricity) because, with the absence of energy gap, the contributions of electrons and holes to the Seebeck coefficient cancel each other [9]. The Seebeck coefficients in metals and semimetals are typically around 80–100 μV/K, while those in semiconductors can be on the order of 10^3 μV/K. However, some recent works have shown that the NLS phases found in Nb_3GeTe [10] or $YbMnSb_2$ [11] might be promising for TE applications with a double value of Seebeck coefficient of normal metals. Motivating by these findings, we are intrigued to systematically investigate the TE properties of type-I and type-II NLSs within the two-band model using the linearized Boltzmann transport theory and relaxation time approximation. We also seek the band parameters that will optimize the TE performance of our model material as characterized by the power factor *PF* and figure of merit *ZT*, defined as [12]

$$PF = S^2\sigma \quad (1)$$

* Corresponding author.
E-mail address: jyesta.ma@gmail.com

$$ZT = \frac{S^2\sigma}{\kappa}T \quad (2)$$

where S is the Seebeck coefficient, σ is the electrical conductivity, κ is the thermal conductivity, and T is the temperature.

THEORETICAL METHODS

We calculate the TE properties using the Boltzmann transport theory with relaxation time approximation. In this approach, the TE transport coefficients (Seebeck coefficient, electrical conductivity, and electron thermal conductivity) can be expressed in terms of the TE integral L_i as [9, 13]

$$S = \frac{1}{eT}\frac{\mathcal{L}_1}{\mathcal{L}_0} \quad (3)$$

$$\sigma = e^2\mathcal{L}_0, \quad (4)$$

and

$$\kappa_e = \frac{1}{T}\left(\mathcal{L}_2 - \frac{\mathcal{L}_1^2}{\mathcal{L}_0}\right), \quad (5)$$

where L_i depends on the transport properties of the material according to

$$\mathcal{L}_i = \int \tau v^2 g(E)\left(-\frac{\partial f}{\partial E}\right)(E-\mu)^i dE\ . \quad (6)$$

In Eq. (6), $v = \hbar^{-1}|\nabla_{\mathbf{k}}E|/\sqrt{3}$ is the electron longitudinal velocity, $f(E)$ is the Fermi Dirac distribution function,

$$f(E) = \frac{1}{1+\exp[(E-\mu)/k_BT]}, \quad (7)$$

and $g(E)$ is the density of states. For the two-band model employed in this paper, the TE integral can be decomposed into a sum of conduction band and valence band contributions, i.e.,

$$\mathcal{L}_{c,i} = \int_{E_{0,c}}^{\infty} \tau v^2 g(E)\left(-\frac{\partial f}{\partial E}\right)(E-\mu)^i dE \quad (8)$$

and

$$\mathcal{L}_{v,i} = \int_{-\infty}^{E_{0,v}} \tau v^2 g(E)\left(-\frac{\partial f}{\partial E}\right)(E-\mu)^i dE, \quad (9)$$

where $E_{0,c}$ and $E_{0,v}$ denote the energy at the band edge of the conduction band and of the valence band, respectively. Following this division, the TE properties of our material can also be decomposed into conduction and valence band components, (denoted by c and v subscript respectively), such that the total TE transport coefficients are given by

$$S = \frac{S_c\sigma_c + S_v\sigma_v}{\sigma_c + \sigma_v}, \quad (10)$$

$$\sigma = \sigma_c + \sigma_v, \quad (11)$$

and

$$\kappa_e = \frac{\sigma_c\sigma_v}{\sigma_c+\sigma_v}(S_c - S_v)^2 + (\kappa_{e,c} + \kappa_{e,v}). \quad (12)$$

We will apply these equations for our model of type-I and type-II NLSs.

Type-I NLS

In the type-I nodal NLS, the nodal line is formed from the crossing of conduction and valence bands with different slope directions. In our model, we use a linear (Dirac) energy dispersion as the conduction band and a parabolic dispersion as the valence band (Fig 1(a)). The energy dispersion relations are

$$E_c(\mathbf{k}) = \hbar v_F|\mathbf{k}| \quad (13)$$

for the conduction band and

$$E_v(\mathbf{k}) = -\frac{\hbar^2|\mathbf{k}|^2}{2m} + E_0 \quad (14)$$

for the valence band, where v_F is the Fermi velocity of the Dirac band, m is the hole effective mass at the band edge, and E_0 is an energy parameter that determines the position of the valence band edge with respect to $E = 0$.

The density of states and longitudinal velocity for the conduction band are given by

$$g_v(E) = \frac{E^2}{\pi^2\hbar^3 v_F^3} \quad (15)$$

and

$$v(E) = \frac{v_F}{\sqrt{3}}, \quad (16)$$

respectively, while for the valence band we have

$$g_v(E) = \frac{m}{\hbar^2\pi^2}\sqrt{\frac{2m(E_0-E)}{\hbar^2}} \quad (17)$$

and

$$v(E) = -\frac{1}{\sqrt{3}}\sqrt{\frac{2(E_0-E)}{m}}. \quad (18)$$

Substituting these parameters to the TE integrals, we obtain

$$\mathcal{L}_{c,i} = \frac{(k_BT)^{i+2}}{3\pi^2\hbar^3 v_F}\int_0^{\infty}\tau(x+\eta)^2 x^i \frac{e^x}{(e^x+1)^2}dx, \quad (19)$$

and

$$\mathcal{L}_{v,i} = \frac{2(k_BT)^{i+3/2}\sqrt{2m}}{3\pi^2\hbar^3} \int_{-\infty}^{\varepsilon_0}\tau(-x-\eta+\varepsilon_0)^{3/2}x^i\frac{e^x}{(e^x+1)^2}dx, \quad (20)$$

where $\eta = \mu/k_BT$ and $\varepsilon_0 = E_0/k_BT$ are the reduced chemical potential and dimensionless band edge position.

Type-II NLS

For the type-II NLS , the crossing between the valence and conduction bands occurs when their slopes have the same direction. We model the type-II NLS using a Dirac conduction band and a Mexican-hat shaped valence band (Fig. 1.(b)). The energy dispersion of the valence band is given by [14, 15]

$$E_v(\mathbf{k}) = -\frac{(\hbar^2k^2/4m - E_1)^2}{E_1} + E_0 \quad (21)$$

Here the parameter E_1 signifies the depth of the central valley of the Mexican-hat band measured from the band edge. The longitudinal velocity and density of states are given by

$$v_\pm(\varepsilon) = \mp\sqrt{\frac{k_BT(\varepsilon_0-\varepsilon)}{3m}}\sqrt{1 \pm \sqrt{(\varepsilon_0-\varepsilon)/\varepsilon_1}} \quad (22)$$

and,

$$g_\pm(\varepsilon) = \frac{4m}{\pi^2\hbar^2}\sqrt{\frac{mk_BT\varepsilon_1}{\hbar^2}}\sqrt{\frac{1 \pm \sqrt{(\varepsilon_0-\varepsilon)/\varepsilon_1}}{(\varepsilon_0-\varepsilon)/\varepsilon_1}} \quad (23)$$

respectively. The ± sign shows two possible values for v, with $-\infty < \varepsilon < \varepsilon_0$ for v_+ and $g_+(\varepsilon)$ (outer ring) and $\varepsilon_1 - \varepsilon_0 < \varepsilon < \varepsilon_0$ for v_- and $g_-(\varepsilon)$ (inner valley). Substituting the longitudinal velocity and density of states into the TE integrals, we obtain

$$\mathcal{L}^{\text{out}}_{v,i} = \frac{4(k_BT)^{i+3/2}\sqrt{m}}{3\pi^2\hbar^3} \int_{-\infty}^{\varepsilon_0-\eta} \tau\varepsilon_1\sqrt{\varepsilon_0-x-\eta}\left(1+\sqrt{(\varepsilon_0-x-\eta)/\varepsilon_1}\right)^{3/2} \frac{e^x}{(e^x+1)^2}x^i dx \quad (24)$$

for the outer ring and

$$\mathcal{L}^{\text{in}}_{v,i} = \frac{4(k_BT)^{i+3/2}\sqrt{m}}{3\pi^2\hbar^3} \int_{\varepsilon_0-\varepsilon_1-\eta}^{\varepsilon_0-\eta} \tau\varepsilon_1\sqrt{\varepsilon_0-x-\eta}\left(1-\sqrt{(\varepsilon_0-x-\eta)/\varepsilon_1}\right)^{3/2} \frac{e^x}{(e^x+1)^2}x^i dx \quad (25)$$

for the inner ring. Here we also scale the chemical potential μ and the energy E_0, E_1 parameters with the thermal energy k_BT, i.e., $\eta = \mu/k_BT$, $\varepsilon_0 = E_0/k_BT$, and $\varepsilon_1 = E_1/k_BT$.

RESULTS AND DISCUSSION

To obtain the TE properties of our model materials, we numerically evaluate the integrals in Eqs. (19), (20), (24), and (25) using the SciPy Python package [16]. We take the temperature T = 300K such that k_BT = 0.026eV. The band shape parameters m and v_F are obtained by fitting our model to the band structure of the type-II NLS Mg_3Bi_2 [7, 8], calculated using the available energy dispersion data from the AFLOWLIB repository [17, 18].

In all our calculations we take $\hbar v_F$ = 0.73 eV Å^{-2} and $\hbar^2/2m$ = 0.104 eV Å^{-2}. We normalize the E_0 and E_1 parameters in terms of k_BT, while the resulting TE transport coefficients are expressed in terms of the constants $S_0 = k_B/e$ = 86.17 μV/K, $\sigma_0 = \frac{2\tau e^2 k_BT}{3\pi^2\hbar^2}\sqrt{2mk_BT/\hbar^2} \approx 10^2$S/m and $\kappa_0 = \frac{2\tau k_B^3T^2}{3\pi^2\hbar^2}\sqrt{2mk_BT/\hbar^2} \approx 10^{-2}$W/m.K.

We also assume the relaxation time to be energy independent (i.e. constant) which is adequate for a lot of cases [19] as this is a common approach in first principles calculations of TE properties such as in the BoltzTraP software package [20].

Type-I NLS

We plot the Seebeck coefficient, electrical conductivity, and electron thermal conductivity for three different values of ε_0 in Fig. 2. We see that the presence of both electron and holes around the nodal lines leads to a low Seebeck coefficient overall due to charge cancellation. Shifting the position of the valence band up further reduces the Seebeck coefficient as this increases the presence of opposing charge carriers both for electron and hole transport. Shifting the position of the valence band also increases the overlap between bands which increases the electrical and thermal conductivity. This increase in electrical conductivity further suppress the Seebeck coefficient, as can be seen from Eqs. (3) and (4).

From here we can obtain the power factor and figure of merit and plot them in Fig. 3. For simplicity, we ignore the phonon thermal conductivity in our calculation. We see a similar trend with the Seebeck coefficient: increasing ε_0 lowers the power factor and figure of merit of the material as the decrease in Seebeck coefficient overwhelms the increase in electrical conductivity. This effect is particularly noticeable for the figure of merit as the increase in electrical conductivity is counteracted by the proportional increase in electron thermal conductivity. We see that the figure of merit of type-I NLS is quite unimpressive, even without including the phonon thermal conductivity. While this "normal" result is expected for a metallic material, perhaps a better TE performance can be obtained with a different band structure, such as one with a flat nodal line portion or with a Mexican-hat shaped band as we will describe in the next section.

Type-II NLS

Now we plot the TE transport coefficients of type-II NLS in Fig. 4. In Figs. 4(a)–(c), we vary the band position ε_0 while keeping the valence band valley depth ε_1 at a constant value of 0.8, which corresponds to the valley depth of Mg_3Bi_2 obtained from density functional theory calculation. Here we might see the results are similar to those in the previous section where increasing ε_0 decreases the Seebeck coefficient and increases the conductivities. However, relative to the type-I NLS, we obtain higher values for all the TE properties in type-II NLS.

In the type-II NLS, the higher Seebeck coefficient, which can be larger than twice that for the normal metals, is most likely due to a jump in the density of states at the edge of the Mexicanhat band and near the edge of the valley. It is well-known that the Mexican hat or ring-shaped bands exhibit such a jump in the density of states [14]. As we can see from Eq. (23), there is a singularity in the density of states when $\varepsilon = \varepsilon_0$, while in the type-I NLS the density of states goes to zero as $\varepsilon = \varepsilon_0$ [Eq. (17)]. Other than the density of states, the higher group velocity for the Mexican-hat band (as $E \propto k^4$) also contributes to an increase in the electrical and thermal conductivities. In Fig. 4(d)–(f) we vary the valley depth ε_1 while keeping ε_0 constant. We see that increasing ε_1 improves both the Seebeck coefficient and the electrical conductivity of type-II NLS, if only slightly, as increasing the valley depth also increases the density of states around the valley.

Turning our attention to the power factor and figure of merit in Fig. 5, we see that the power factor and figure of merit of type-II NLS are significantly larger than those of type-I NLS. Interestingly, we see in Fig. 5(c) that the slight increase in Seebeck coefficient and electrical conductivity from increased ε_1 translates to a significant increase in the power factor. The figure of merit [Fig. 5(d)] also improves with increasing ε_1 although it is not remarkable since the increase in electrical and electron thermal conductivity cancels each other. Thus, we may obtain the highest TE performance when the valence band edge (in this case, the valley) is as close as possible to the conduction band edge. Note that, however, ε_1 cannot be increased indefinitely because when $\varepsilon_1 \geq \varepsilon_0$ the band crossing vanishes and we no longer have a nodal line semimetal.

CONCLUSION

While the TE performance of type-I NLS is not extraordinary, the type-II NLS exhibits a remarkable improvement in the Seebeck coefficient and figure of merit compared to the normal metals. We obtain the best TE performance when the position of the valence band is close to the conduction band edge. For the type-II NLS with a Mexican-hat band, increasing the valley depth improves the power factor significantly. Further research in this area is required to discover a candidate of type-II NLS material with good thermoelectric properties. Learning from the discovery of Mg_3Bi_2 [7, 8], we suggest that combining a light element in the alkaline earth metals family and a heavy element in the pnictogens family might be a promising direction for finding the potential type-II NLS as a high-performance TE material.

ACKNOWLEDGMENT

J.M.A and B.E.G. acknowledge funding from P2MI ITB 2021.

REFERENCES

[1] N. P. Armitage, E. J. Mele, and A. Vishwanath, *Rev. Mod. Phys.*, **90,** 015001, 2018
[2] P. Liu, J. R. Williams, and J.J. Cha, *Nat. Rev. Mater.*, **4**, 479–496, 2019
[3] J. Zou, Z. He, and G. Xu, *Npj Comput. Mater.*, **5,** 96, 2019
[4] S. Li, et. al., *Front. Phys. (Lausanne)*, **15,** 43201, 2020
[5] A. Burkov, *Nature Mater.*, **15,** 1145–1148, 2016
[6] C. Fang, et. al., *Chin. Phys. B.*, **25,** 117106, 2016
[7] T. R. Chang, et. al., *Adv. Sci.,* **6,** 1800897, 2019
[8] X. Zhang, et. al., *J. Phys. Chem. Lett.*, **8,** 4814–4819, 2017
[9] E.H. Hasdeo, et. al., *J. Appl. Phys.*, **126,** 035109, 2019
[10] X. Wang, et. al., *Nanoscale*, **12,** 16910–16916, 2020
[11] Y. Pan, et. al., *Adv. Mater.*, **33,** 2003168, 2021
[12] H.J. Goldsmid, *Introduction to Thermoelectricity*, Berlin: Springer-Verlag, 2010
[13] N. Ashcroft and D. Mermin *Solid State Physics*, Orlando: Harcourt, 1976
[14] D. Wickramaratne, F. Zahid, and R. K. Lake, *J. Appl. Phys.*, **118,** 075101, 2015
[15] M. Nurhuda, et. al., *Adv. Nat. Sci-Nanosci* **11,** 015012, 2020
[16] P. Virtanen, et. al., *Nat. Methods*, **17,** 261–272, 2020
[17] S. Curtarolo, et. al., *Comput. Mater. Sci.*, **58** 218–226, 2020
[18] S. Curtarolo, et. al., *Comput. Mater. Sci.*, **58,** 227–235, 2020
[19] D. Singh, *Phys. Rev. B*, **81,** 195217, 2010

[20] G. K. H. Madsen, J. Carrete, and M.J. Verstraete, *Comput. Phys. Commun.*, **231,** 140–145, 2018

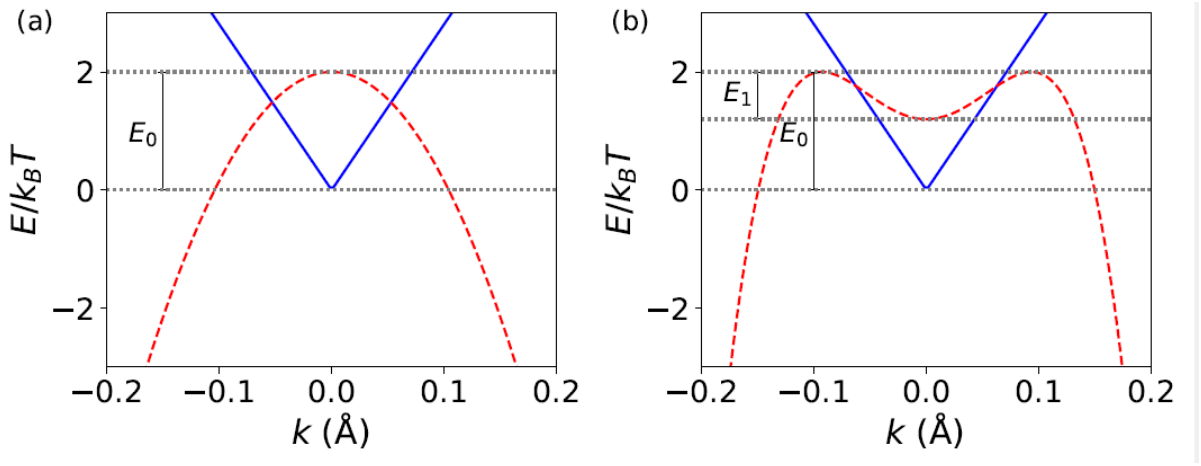

Fig. 1**.** The model band structure for (a) type-I and (b) type-II NLSs. Here we take $E_0 = 2k_BT$ and $E_1 = 0.8k_BT$

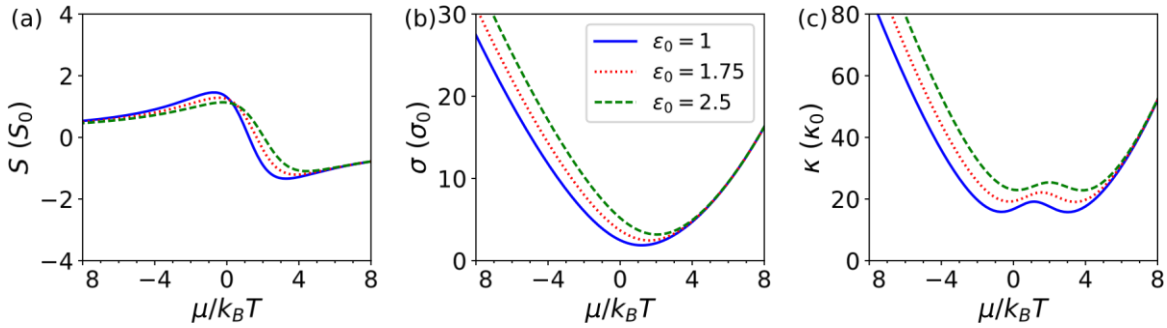

Fig. 2. Thermoelectric transport coefficients in a type-I NLS with a varying value of $\varepsilon_0 = E_0/k_BT$. (a) Seebeck coefficient, (b) electrical conductivity, and (c) electron thermal conductivity, plotted as a function of chemical potential.

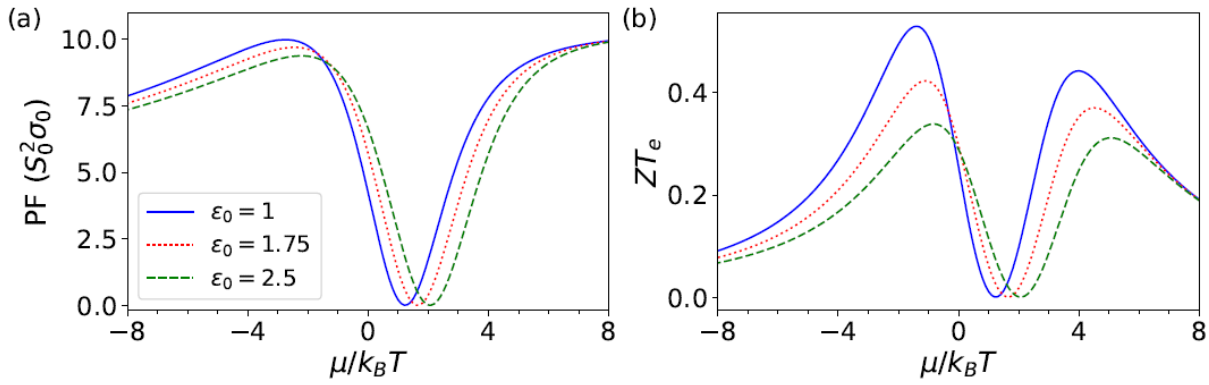

Fig. 3. Thermoelectric performance of type-I NLS. (a) Power factor and (b) ideal figure of merit, plotted as a function of chemical potential.

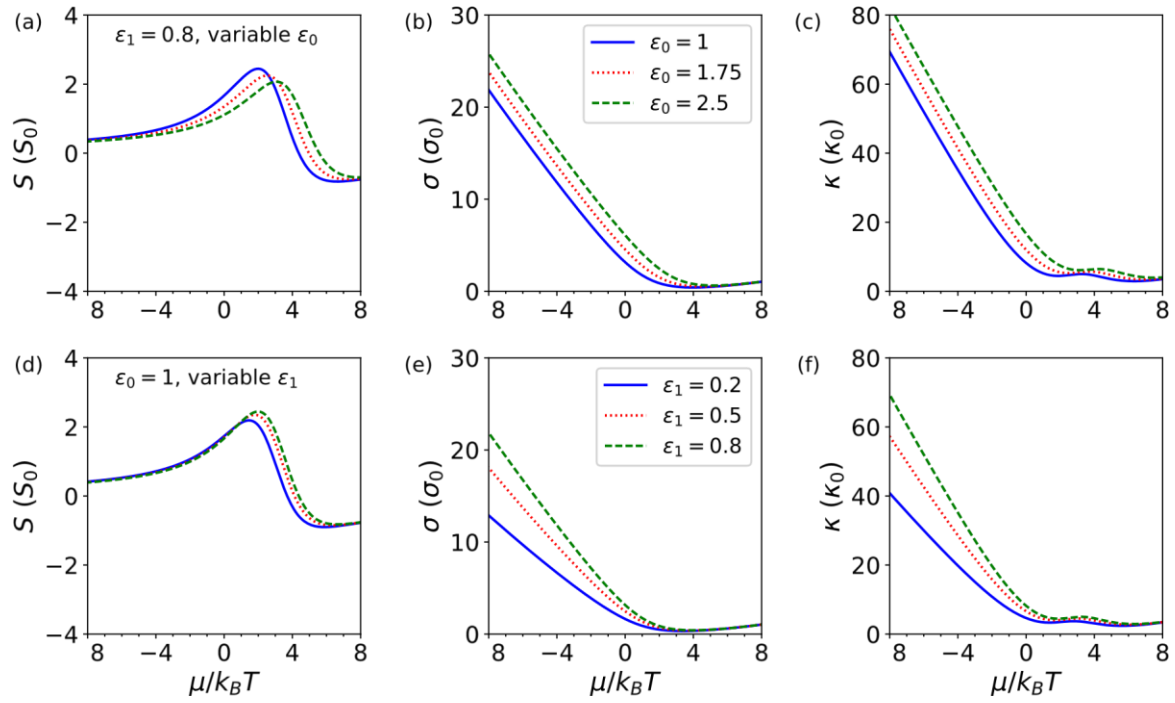

Fig. 4. The Seebeck coefficient, electrical conductivity, and electron thermal conductivity for a type-II NLS with a constant $\varepsilon_1 = 0.8$ and varying ε_0 in panels (a)–(c), compared to the cases of using a constant $\varepsilon_0 = 1$ and varying ε_1 in panels (d)–(f).

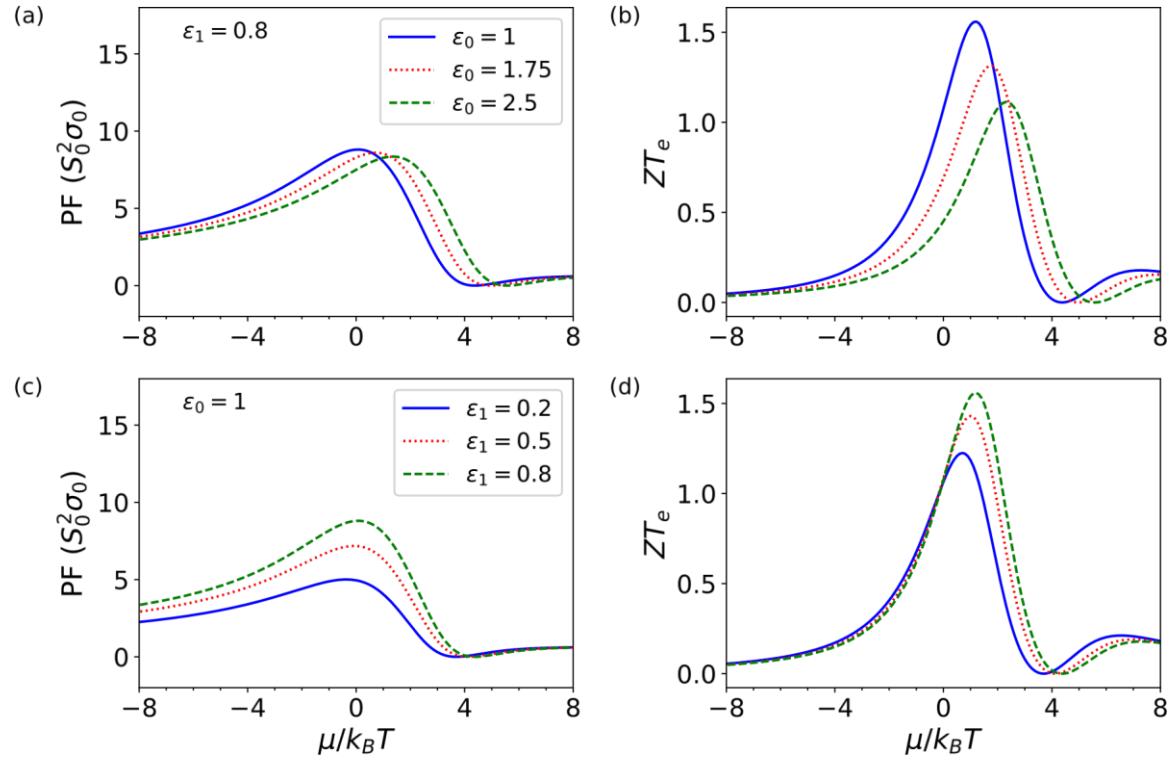

Fig. 5. The power factor and ideal figure of merit for a type-II NLS with a fixed $\varepsilon_1 = 0.8$ and varying ε_0 in (a)–(b) and with a fixed $\varepsilon_0 = 1$ and varying ε_1 in (c)–(d).